CEREBROVASCULAR LANDMARK DETECTION UNDER ANATOMICAL VARIATIONS

Zimeng Tan[1,2], *Jianjiang Feng*[1,2(✉)], *Wangsheng Lu*[3], *Yin Yin*[3], *Guangming Yang*[3], *and Jie Zhou*[1,2]

[1] Department of Automation, Tsinghua University, Beijing, China

[2] Beijing National Research Center for Information Science and Technology, Beijing, China

[3] UnionStrong (Beijing) Technology Co.Ltd, Beijing, China

ABSTRACT

Anatomical landmark detection has important applications in cerebrovascular analysis and clinical treatments, which is challenging due to the complex structure, various natural variations and pathological changes. In this paper, we propose a multi-task deep learning network for accurate detection of 19 landmarks in cerebral Magnetic Resonance Angiography (MRA) images, which is robust to anatomical variations. Besides landmark detection, the network is trained to perform landmark attribute classification, semantic artery segmentation and arterial segment attribute classification simultaneously. The attributes of landmark and arterial segment are defined as local bifurcation appearance and absence variation, respectively, which enhances the contextual information and incorporates the structural prior knowledge explicitly. Experiments on both public and private datasets demonstrate the superior performance of the proposed method.

Index Terms— Cerebrovascular landmark detection, multi-task, anatomical variations, attribute classification

1. INTRODUCTION

Cerebrovascular diseases, such as aneurysms and stenosis, have become one of the most serious diseases threatening human health in the world [1]. Anatomical landmark detection plays an important role in cerebrovascular analysis and clinical treatments, which models the vascular hierarchical topology explicitly and provides essential structural knowledge for subsequent medical image processing, such as centerline labeling [2] and vascular network registration between different periods or different subjects [3]. In this paper, we focus on the Circle of Willis (CoW) in cerebral MRA images, which has a high incidence of vascular diseases [4] and can normally be divided into 20 arterial segments according to 19 bifurcation landmarks [5] (see Fig. 1(a) and (b)). There are many physiological variations in CoW, including loss of one or multiple arterial segments [6] (see Fig. 1(c) and (d)). The detection of landmarks at both ends of missing arterial segment is particularly difficult, which always relies on spatial symmetry and clinical experience in manual annotation. In addition, disease

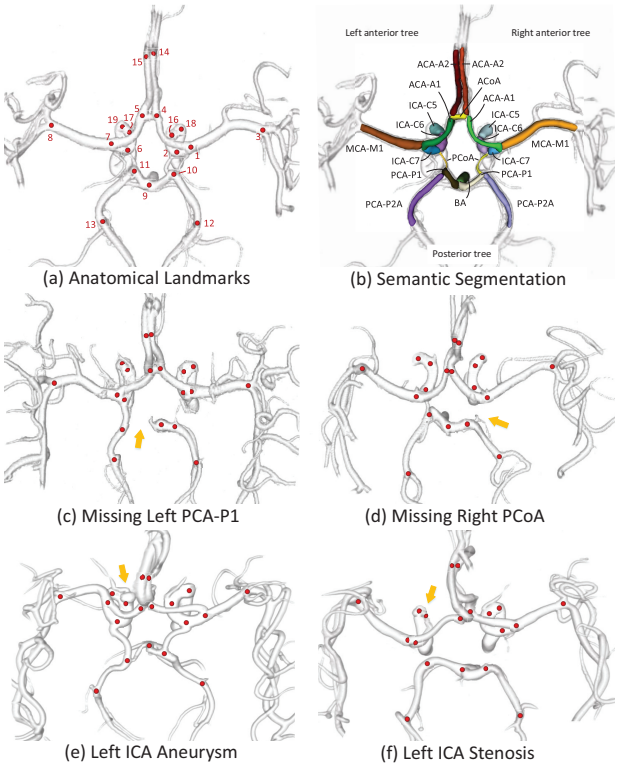

Fig. 1. Illustration of (a) anatomical landmarks, (b) semantic segmentation, (c,d) natural variations, and (e,f) pathological changes of cerebrovascular.

related changes of vessels are also challenging. For example, aneurysm and stenosis cause mutations in vascular diameter and change the local blood flow velocity, blurring the vascular appearance in MRA images (see Fig. 1(e) and (f)).

There have been numerous efforts for anatomical landmark detection, and remarkable success was achieved using encoder-decoder network based heatmap regression methods [7–13]. Compared with predicting absolute landmark coordinates directly, these voxel-wise heatmap regression approaches are intrinsically more suitable for landmark detection, as they focus on each position. Meanwhile, many deep learning-based methods have been developed for cere-

(a) Right PCoA (b) Missing Right PCoA

Fig. 2. Arterial segment variation and related changes of local bifurcation appearance around corresponding landmarks.

brovascular analysis, such as segmentation [14–19], arterial labeling [2, 20] and lesion detection [21]. Although yielding promising predictions, little attention has been paid to cerebrovascular landmark localization, which is still a challenging problem due to the complex structure and various variations.

Recently, multi-task framework has been widely explored in many domains, including medical segmentation [22] and disease diagnosis [23], which demonstrates that leveraging the synergy among different tasks could boost the individual performance. In this paper, we propose an variation-robust multi-task network for accurate cerebrovascular landmark detection in MRA images. Similar to [13], we introduce vascular semantic segmentation as auxiliary objective. The label of semantic segmentation is defined by dividing the vascular binary segmentation according to the landmark distribution. In this way, the semantic segmentation task is highly correlated with landmark detection, which enhances the contextual information and incorporates structural prior explicitly. Differently from [13], considering that anatomical variations are very common in cerebrovascular, we further perform attribute classification of landmarks and arterial segments in parallel. Obviously, when the CoW is complete, all landmarks are located at vascular bifurcations. While there is a missing arterial segment, the landmarks at both ends will not have local forked appearance. Therefore, there is a corresponding relationship between landmark attribute (i.e., whether has local bifurcation characteristics) and arterial segment attribute (i.e., whether exists). Constraining the outputs of two classification tasks guides the network to obtain self-consistent predictions.

In summary, the main contribution of this work is threefold. Firstly, we propose a multi-task network for automatic and accurate cerebrovascular landmark detection in MRA images, which is robust to anatomical variations. Secondly, we introduce anatomical landmark and arterial segment attribute classification tasks, which reflect the vascular anatomical variations and local bifurcation appearance changes of related landmarks. A self-consistency loss function is applied to supervise the rationality of two attribute predictions. Thirdly, extensive experiments on both public and private datasets demonstrate the effectiveness and robustness of the proposed method. The manual landmark annotations of 40 public MRA images will be released to promote further study.

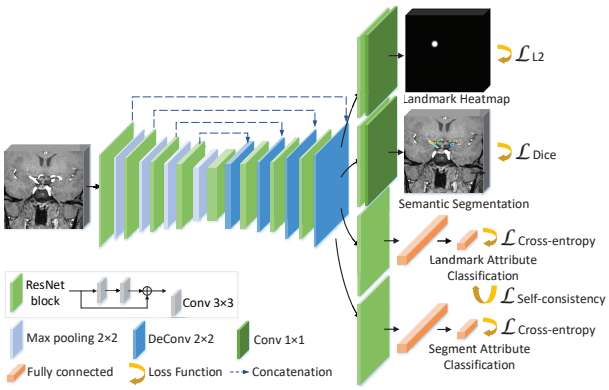

Fig. 3. Overview of the proposed framework.

2. METHODS

2.1. Attributes of Landmarks and Arterial Segments

Compared with other anatomical tubular structures, such as airway and aorta, the biggest challenge of cerebrovascular landmark detection is that natural variations are very common. How to model and deal with the problem of missing arterial segments is a key issue in cerebrovascular analysis. Note that in this paper, we hypothesis that all the landmarks exist regardless of the vascular variations. When a certain arterial segment is missing, the local appearance of landmarks at both ends will be affected. For example, when the right PCoA exists (see Fig. 2(a)), the landmark A and B at both ends have forked appearance. However, when the right PCoA is missing (see Fig. 2(b)), A and B are located at the smooth arterial segments with no local bifurcation. We regard the vascular absence and related changes of bifurcation characteristics as additional attributes of the arterial segment and landmark, respectively, and convert attribute computation to classification problems. That is, the network is trained to judge whether each arterial segment exists and whether there is a local bifurcation at each landmark position simultaneously. In this way, the cerebrovascular variations can be associated with landmark detection explicitly. The anatomical prior and structural information are incorporated at the same time.

Furthermore, although feature representations can be shared between two attribute classification tasks, the rationality of the outputs still needs to be supervised. That is, the two attribute predictions should be self-consistent. Note that in common physiological variations, only part of the arterial segments may be missing (e.g., ACoA, PCoA, PCA-P1, and ACA-A1), and only the attributes of the related landmarks may be changed. Specifically, we assume that prediction of the arterial segment attribute is more intuitive and robust. For segment attribute prediction y_s, the corresponding landmark attribute $\tilde{y}_l$ can be derived. Then we apply a cross-entropy

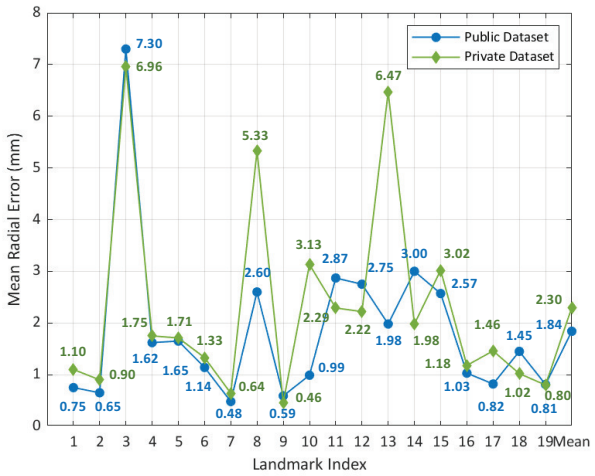

Fig. 4. Quantitative results on both public and private test sets. Performance is measured using MRE (in mm).

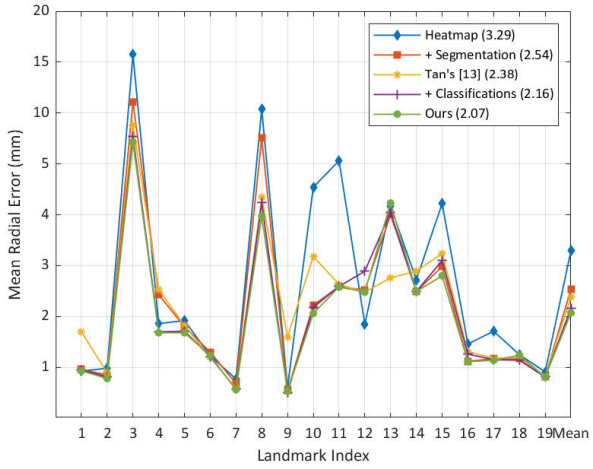

Fig. 5. Comparison of network architectures with different auxiliary task configurations on all 20 testing data, where the mean MRE is marked in the legend (in mm). Y-axis is non-linear for better visualization.

loss function between $\tilde{y}_l$ and landmark attribute prediction y_l:

$$\mathcal{L}_{self} = -\sum_{i \in \Theta} \tilde{y}_l^i \log(y_l^i) \tag{1}$$

where the superscript i represents the ith landmark, and Θ denotes the set of landmarks whose attributes may be changed due to the arterial segment absence. The proposed self-consistency loss function supervises the uniform of the two attribute classification predictions, which leads the network to be more sensitive of the local appearance around landmarks.

2.2. Multi-Task Framework

We propose a multi-task framework for landmark detection, where the cerebrovascular semantic segmentation, landmark and arterial segment attribute classification are introduced as auxiliary tasks. The detailed architecture is illustrated in Fig. 3. Inspired by [7], we convert landmark detection to a heatmap regression task. Each landmark has a separate volumetric output where a Gaussian spot centered at the landmark position. The heatmap $G_i(x)$ of voxel x ranges in [0,1], which represents the probability to be the ith landmark and is determined by the distance from voxel x to the ith landmark position x_i. More formally, the heatmap is defined as:

$$G_i(x) = e^{-\frac{1}{2\delta^2}(x-x_i)^2}, i = 1, 2, ..., 19. \tag{2}$$

where the standard deviation δ controls the size of distribution. During inference, we derive the landmark position by performing the argmax operation on the heatmap prediction.

The cerebrovascular semantic segmentation task is considered as a voxel-wise multi-class classification problem, where arterial segments are regarded as different semantic classes. In preparing semantic segmentation ground truth, the arterial segments are divided from the binary segmentation around the CoW. That is, the landmark is located at the center of the interface between adjacent segments. By emphasizing the different arterial segments, we enhance the contextual information and provide more feature representations for learning structural prior knowledge.

We exploit a modified U-Net [24] as our backbone in the proposed multi-task framework. The plain convolution layer is replaced by ResNet block [25] to avoid gradient vanishing, which contains two convolution operators and a shortcut connection between input and output. The skip connection between encoder and decoder path incorporates the low-level fine features with the high-level abstract features, preserving more spatial details for better localization. Then the network is split into four parallel branches to complete different tasks simultaneously. By sharing the same extracted features, the network learns a joint representation among landmark detection, semantic segmentation, and attribute classification tasks. The synergy among them guides the network to capture more discriminative features and boosts the final performance.

We apply L2 loss, Dice loss and cross-entropy loss functions for landmark heatmap regression, semantic segmentation and attribute classification tasks, respectively. To address the class imbalance problem, we weighted the L2 loss and Dice loss functions according to the voxel number ratio of the background to each kind of foreground class. The final objective is defined as a linear combination of all loss functions.

3. EXPERIMENTS

3.1. Datasets and Implementation Details

We evaluated the proposed method on both public and private datasets. The public dataset is comprised of 40 healthy

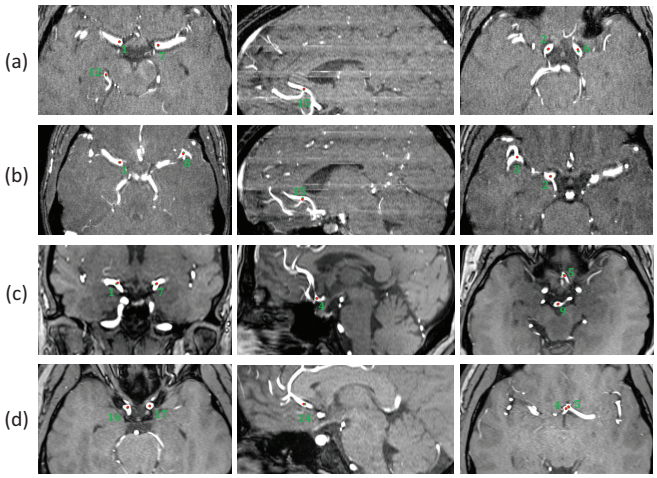

Fig. 6. Visualization of landmark detection results. (a,b) images from public dataset; (c,d) images from private dataset.

cerebral MRA volumes randomly selected from UNC dataset (https://public.kitware.com/Wiki/TubeTK/Data), which contains 109 images totally. The private dataset contains 40 clinically collected MRA images with aneurysms or stenosis. For each volume, 19 anatomical landmarks and binary segmentation around the CoW region were annotated manually first by one of the authors and then verified by an experienced neurosurgeon. The landmark annotations of the public dataset will be released. The semantic segmentation label was established based on the binary segmentation and landmark distribution, followed by manual correction. Then the attributes of landmarks and arterial segments were determined accordingly. We performed intensity-based rigid registration by taking a training sample as template firstly, and all images were spatially normalized to $0.513\times0.513\times0.8$ mm^3. Each dataset was split randomly into a training set (25 images), a validation set (5 images), and a testing set (10 images). The network was trained using all 50 training images jointly.

Considering the initial coarse registration, only random translation was applied for data augmentation. The whole framework was implemented in TensorFlow. We trained the proposed network using Adam optimizer ($\beta_1 = 0.5, \beta_2 = 0.999$) with the learning rate of 0.0001 for 150 epochs.

3.2. Results

We utilize the mean radial error (MRE, in mm) as the metric to evaluate our method, which refers to the mean Euclidean distance between the ground truth and predicted landmark positions. The quantitative results, as shown in Fig. 4, demonstrate that the proposed method achieves excellent performance on both public and private datasets. Some landmarks are challenging intrinsically due to the complex structure and show higher detection error. For example, there may be mulitple extra branches in the MCA segment, and the landmarks between M1 and M2 segments (i.e., landmark 3 and 8) may be misidentified as other bifurcations. Fig. 6 shows some typical results, where the ground truth and predicted positions are represented with green and red dots. For auxiliary objectives, the mean Dice coefficient of the semantic segmentation is 54.25%, mainly because of the curvilinear structure and unobvious class interface, which will be explored in the future. The classification accuracy of landmark and arterial segment is 88.95% and 97.25%, respectively.

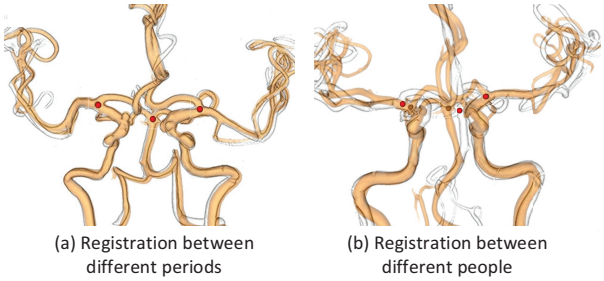

Fig. 7. Cerebrovascular registration using landmark predictions between (a) different periods and (b) different people, where the data shown in orange represents the template.

To verify the components of the proposed mechanism, we conduct ablation experiments on all 20 testing data. We compare the performance of the backbone network with different task configurations. As shown in Fig. 5, adding each of auxiliary tasks successively brings better overall results. Note that the network with only heatmap regression task is similar to [7], where the backbone network is replaced by a modified U-Net. We also compare our method with [13], which exploits semantic segmentation and orientation field regression as auxiliary tasks. The experimental results demonstrate the effectiveness and robustness of the proposed method, especially for clinically significant landmarks.

Furthermore, as shown in Fig. 7, we illustrate cerebrovascular registration results using landmark predictions between different periods and different people, which is beneficial for disease progression tracking and population analysis.

4. CONCLUSION

In this paper, we have proposed an multi-task network for cerebrovascular landmark detection in MRA images, which is robust to anatomical variations. Semantic segmentation, attribute classifications of landmark and arterial segment are introduced as auxiliary objectives to guide the network to learn more discriminative features. We defined the attributes of the landmark and arterial segment as local bifurcation appearance and absence variation, respectively, incorporating the contextual information and structural prior explicitly. Experiments on both public and private datasets demonstrate the effectiveness of the proposed framework. In the future, we will extend our method to other anatomical tubular structures.

5. COMPLIANCE WITH ETHICAL STANDARDS

This study got ethical approval of Xuanwu Hospital of Capital Medical University (2020009) for using the clinically collected cerebral MRA dataset. The UNC dataset is publicly available.

References

[1] Marin Yasugi et al., "Relationship between cerebral aneurysm development and cerebral artery shape," *JACIII*, vol. 22, no. 2, pp. 249–255, 2018.

[2] Li Chen et al., "Automated intracranial artery labeling using a graph neural network and hierarchical refinement," in *MICCAI*, 2020, pp. 76–85.

[3] Sepideh Almasi et al., "Cerebrovascular network registration via an efficient attributed graph matching technique," *MedIA*, vol. 46, pp. 118–129, 2018.

[4] Tom van Seeters et al., "Completeness of the circle of willis and risk of ischemic stroke in patients without cerebrovascular disease," *Neuroradiology*, vol. 57, no. 12, pp. 1247–1251, 2015.

[5] Hrvoje Bogunović et al., "Anatomical labeling of the circle of willis using maximum a posteriori probability estimation," *MedIA*, vol. 32, no. 9, pp. 1587–1599, 2013.

[6] Fethi Emre Ustabaşıoğlu and Serdar Solak, "Magnetic resonance angiographic evaluation of anatomic variations of the circle of willis," *The Medical Journal Of Haydarpaşa Numune Training and Research Hospital*, vol. 59, no. 3, pp. 291–295, 2019.

[7] Christian Payer, Darko Štern, Horst Bischof, and Martin Urschler, "Regressing heatmaps for multiple landmark localization using CNNs," in *MICCAI*, 2016, pp. 230–238.

[8] Zhusi Zhong et al., "An attention-guided deep regression model for landmark detection in cephalograms," in *MICCAI*, 2019, pp. 540–548.

[9] Runnan Chen et al., "Cephalometric landmark detection by attentive feature pyramid fusion and regression-voting," in *MICCAI*, 2019, pp. 873–881.

[10] Christian Payer, Darko Štern, Horst Bischof, and Martin Urschler, "Integrating spatial configuration into heatmap regression based CNNs for landmark localization," *MedIA*, vol. 54, pp. 207–219, 2019.

[11] Wei Liu et al., "Landmarks detection with anatomical constraints for total hip arthroplasty preoperative measurements," in *MICCAI*, 2020, pp. 670–679.

[12] Yankun Lang et al., "Automatic localization of landmarks in craniomaxillofacial CBCT images using a local attention-based graph convolution network," in *MICCAI*, 2020, pp. 817–826.

[13] Zimeng Tan, Jianjiang Feng, and Jie Zhou, "Multi-task learning network for landmark detection in anatomical tree structures," in *ISBI*, 2021, pp. 1975–1979.

[14] Lei Mou et al., "CS2-Net: Deep learning segmentation of curvilinear structures in medical imaging," *MedIA*, vol. 67, pp. 101874, 2021.

[15] Hao Zhang et al., "Cerebrovascular segmentation in MRA via reverse edge attention network," in *MICCAI*, 2020, pp. 66–75.

[16] Yifan Wang et al., "Jointvesselnet: Joint volume-projection convolutional embedding networks for 3D cerebrovascular segmentation," in *MICCAI*, 2020, pp. 106–116.

[17] Baochang Zhang et al., "Cerebrovascular segmentation from TOF-MRA using model-and data-driven method via sparse labels," *Neurocomputing*, vol. 380, pp. 162–179, 2020.

[18] Pedro Sanchesa et al., "Cerebrovascular network segmentation of MRA images with deep learning," in *ISBI*, 2019, pp. 768–771.

[19] Shoujun Zhou et al., "Statistical intensity-and shape-modeling to automate cerebrovascular segmentation from tof-mra data," in *MICCAI*, 2019, pp. 164–172.

[20] Xingce Wang et al., "Automatic labeling of vascular structures with topological constraints via HMM," in *MICCAI*, 2017, pp. 208–215.

[21] Daiju Ueda et al., "Deep learning for mr angiography: automated detection of cerebral aneurysms," *Radiology*, vol. 290, no. 1, pp. 187–194, 2019.

[22] Xuanang Xu et al., "Asymmetrical multi-task attention U-Net for the segmentation of prostate bed in CT image," in *MICCAI*, 2020, pp. 470–479.

[23] Wei Shao et al., "Multi-task multi-modal learning for joint diagnosis and prognosis of human cancers," *MedIA*, vol. 65, pp. 101795, 2020.

[24] Olaf Ronneberger, Philipp Fischer, and Thomas Brox, "U-Net: Convolutional networks for biomedical image segmentation," in *MICCAI*, 2015, pp. 234–241.

[25] Kaiming He, Xiangyu Zhang, Shaoqing Ren, and Jian Sun, "Deep residual learning for image recognition," in *CVPR*, 2016, pp. 770–778.